Liquid Crystals
Publication details, including instructions for authors and subscription information:
http://www.informaworld.com/smpp/title~content=t713926090

Novel glass-forming liquid crystals. IV. Effects of central core and pendant group on vitrification and morphological stability

Shaw H. Chen[ab]; John C. Mastrangelo[a]; Thomas N. Blanton[c]; A. Bashir-Hashemi[d]; Kenneth L. Marshall[b]
[a] Materials Science Program and Chemical Engineering Department, [b] Laboratory for Laser Energetics, Center for Optoelectronics & Imaging, University of Rochester, Rochester, NY, USA [c] Analytical Technology Division, Eastman Kodak Company, Rochester, NY, USA [d] Geo-Centers, INC. at Armament Research, Development and Engineering Center, Lake Hopatcong, NJ, USA

To cite this Article Chen, Shaw H. , Mastrangelo, John C. , Blanton, Thomas N. , Bashir-Hashemi, A. and Marshall, Kenneth L.(1996) 'Novel glass-forming liquid crystals. IV. Effects of central core and pendant group on vitrification and morphological stability', Liquid Crystals, 21: 5, 683 — 694
To link to this Article: DOI: 10.1080/02678299608032880
URL: http://dx.doi.org/10.1080/02678299608032880

LIQUID CRYSTALS, 1996, VOL. 21, NO. 5, 683–694

Novel glass-forming liquid crystals. IV. Effects of central core and pendant group on vitrification and morphological stability

by SHAW H. CHEN*†‡, JOHN C. MASTRANGELO†, THOMAS N. BLANTON§, A. BASHIR-HASHEMI¶ and KENNETH L. MARSHALL‡

†Materials Science Program and Chemical Engineering Department
‡Laboratory for Laser Energetics, Center for Optoelectronics & Imaging, 240 East River Road, University of Rochester, Rochester, NY 14623-1212, USA
§Analytical Technology Division, Eastman Kodak Company, Kodak Park, BLDG. 49, Rochester, NY 14652-3712, USA
¶Geo-Centers, INC. at Armament Research, Development and Engineering Center, Lake Hopatcong, NJ 07849, USA

(*Received 15 February 1996; in final form 23 May 1996; accepted 25 May 1996*)

To unravel the effects of the volume-excluding central core and the mesogenic pendant group on both the glass-forming ability and morphological stability of the thermally quenched glass, nine model compounds were synthesized that contain various nematogenic and cholesteryl pendant groups. The glass-forming ability of the melt and morphological stability of the thermally quenched glass were assessed using the DSC, XRD, and hot-stage POM techniques. With cyanobiphenyl as the pendant group, the following descending order in morphological stability against thermally activated recrystallization was established: *trans*-cyclohexane > *all-exo*-bicyclo[2.2.2]oct-7-ene > cubane > *cis*-cyclohexane > benzene. While the cyclohexane compound containing three cyanoterphenyl groups showed a strong tendency to crystallize upon quenching, the chiral nematic system in which one of the cyanoterphenyl groups is substituted by a cholesteryl group showed superior glass-forming ability and morphological stability. Additionally, with *cis*-cyclohexane as the central core the angular 6-(4-cyanophenyl)-naphthyl group, a stronger nematogen, showed a comparable glass-forming ability but a superior morphological ability in comparison to the cyanobiphenyl group. However, with *all-exo*-bicyclo[2.2.2]oct-7-ene as the central core, the angular 1-phenyl-2-(6-cyanonaphth-2-yl)ethyne, also a stronger nematogen, turned out to be inferior to the cyanobiphenyl group with respect to morphological stability. It appears that the glass-forming ability and morphological stability of the hybrid system are determined by the characters of both the volume-excluding core and the pendant group, a delicate structural balance between the two constituents, and the stereochemistry of the hybrid system.

1. Introduction

Because of the spontaneous molecular assembly into various mesophases, liquid crystals (LCs) have found numerous established as well as potential optical applications. As traditionally employed in the now mature LC displays, LCs function in the fluid phase in which molecular orientation with an external field is the basis for practical applications. In this case critical requirements are that the LC material have a sub-ambient melting point and that a wide mesomorphic temperature range exists to facilitate applications under a wide range of conditions. In addition, one of the remaining challenges lies in the design of novel LC materials with low melt viscosity and high dielectric anisotropy to ensure fast response and low driving voltage.

*Author for correspondence.

Liquid crystals are also potentially capable of serving a diversity of emerging linear and non-linear optical technologies, such as control of polarization of light [1], optical information storage [2, 3], frequency conversion [5–7], etc, in which molecular orientation in response to an applied field is not essential. In these applications, it is desirable to have a high degree of mesomorphic order frozen in a glassy matrix, resulting in vitrified films that are optically anisotropic. Thus, materials capable of both vitrification and liquid crystalline mesomorphism have been intensively explored in recent years. Two distinct classes of organic materials have emerged as a result: LC polymers (LCPs) with a molecular weight on the order of at least 10^4 g mole^{-1} and glass-forming LCs (GLCs) with a molecular weight $\leqslant 1500$ in general. In view of the relative ease of processing into uniform thin films because of low melt viscosity, we have focused our recent activities on GLCs.

0267–8292/96 $12·00

Although numerous GLCs have been reported in the recent past [8–16], vitrification by organic compounds in general has remained poorly understood from the standpoint of chemical structure. Moreover, the morphological stability against thermally activated phase transformation, for example, recrystallization of a mesomorphic or an isotropic melt, has not been systematically investigated. Based on a molecular design concept in which the mesogenic cores are attached to volume-excluding cores, we have reported a series of GLCs using mostly cyclohexane [17–19] and, in one instance, adamantane [20] as the volume-excluding cores. Morphological stability of selected GLCs has also been experimentally evaluated via the measurement of spherulitic growth rate [21]. In the present work, GLCs consisting of *cis*- and *trans*-cyclohexane, *all-exo*-bicyclo[2.2.2]oct-7-ene, and cubane with various pendant groups were synthesized and their morphological stability characterized by differential scanning calorimetry (DSC), X-ray diffractometry (XRD), and polarized optical microscopy (POM) with an objective of unravelling the effects of both the pendant group and central core on vitrification and morphological stability.

2. Experimental

2.1. *Reagents and chemicals*

All solvents and reagents were purchased from the Aldrich Chemical Company or J. T. Baker: methylene chloride (>99·5 per cent), *N*,*N*-dimethylformamide (99·8 per cent), diethyl ether (99 per cent), acetone (99·7 per cent), benzene (99 per cent), ethanol (denatured), magnesium sulphate (99 per cent), potassium hydroxide (85 per cent, 15 per cent water), caesium carbonate (99 per cent), sodium carbonate (99·5 per cent), ammonium hydroxide (30 per cent aq.), hydrochloric acid (37 per cent aq.), anhydrous pyridine (<0·005 per cent water, 99·8 per cent), 3,4-dihydro-2*H*-pyran (97 per cent), 2-iodoethanol (99 per cent), pyridinium *p*-toluenesulphonate (98 per cent), cholesterol (99 per cent), oxalyl chloride (99 per cent), tetrakis(triphenylphosphine)palladium(0) (99 per cent), 3-bromo-1-propanol (97 per cent), 6-bromo-2-naphthol (97 per cent), 4-hydroxy-4′-bromobiphenyl (97 per cent), diethyl azodicarboxylate (97 per cent), triphenylphosphine (99 per cent), bicyclo[2.2.2]oct-7-ene-2,3,5,6-tetracarboxylic dianhydride, *cis*-1,3,5-cyclohexanetricarboxylic acid (95 per cent), 1,3,5-benzenetricarboxylic acid (98 per cent), dimethyl 1,4-bis(methoxycarbonyl)cubane (99 per cent), and silica gel (40 μm flash chromatography packing). Tetrahydrofuran (99 per cent) was dried by refluxing over sodium in the presence of benzophenone until blue; the solvent was then collected via distillation.

2.2. *Material synthesis*

Model compounds (**I**) to (**IX**), as depicted in figure 1, were synthesized for the present study. The alcohol 4-(3-hydroxypropyl)-4′-cyanobiphenyl, a precursor to compounds (**I**), (**II**), (**VI**), (**VII**) and (**VIII**), was prepared following a procedure reported previously [22]. The precursor to (**IX**), 2-[4-(6′-cyanonaphthyl)ethynyl) phenoxy]ethanol, was synthesized as part of a previous study [18], where the synthesis of chiral nematic systems was also presented. Compound (**V**) in the present work was synthesized by way of an acid chloride-anhydride intermediate prepared from 1,3,5-cyclohexanetricarboxylic acid following the same procedure. All the model compounds were synthesized by performing the Mitsunobu reaction between a carboxylic acid and an alcohol except (**V**) and (**VII**).

2.2.1. *2-(3-Hydroxypropyl)-6-(4-cyanophenyl)naphthalene and 4-(3-hydroxypropyl)-4″-cyanoterphenyl*

Synthesis of both alcohols was accomplished following Scheme 1. A mixture of 6-bromo-2-napthol (5·00 g, 22·4 mmol), 3-bromo-1-propanol (4·00 g, 28·8 mmol), and KOH (1·25 g, 18·9 mmol) in 50 ml *N*,*N*-dimethylformamide was stirred at 92°C for 15 h. Upon cooling to ambient temperature, the mixture was poured into 350 ml of diethyl ether followed by washing with water (5 × 100 ml). The organic layer was then evaporated to dryness for purification on a flash silica gel column using methylene chloride/acetone (10 : 1) as the eluent to yield 2-(3-hydroxypropyl)-6-bromonaphthalene (3·70 g, 59 per cent). Another intermediate, 4-cyanophenylboronic acid, was prepared following the procedures reported by Hird *et al.* [23].

A mixture of 2-(3-hydroxypropyl)-6-bromonaphthalene (3·75 g, 13·3 mmol), 4-cyanophenylboronic acid

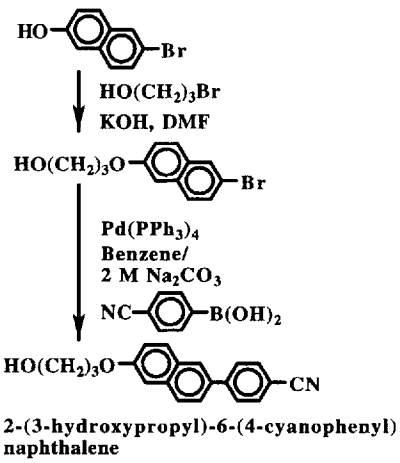

Scheme 1. Synthesis of 2-(3-hydroxypropl)-6-(4-cyanophenyl)-naphthalene.

(2·17 g, 14·8 mmol), tetrakis(triphenylphosphine)palladium(0) (0·44 g, 0·38 mmol), benzene (30 ml), 2 M Na_2CO_3 aqueous solution (30 ml), and 6 ml ethanol (6 ml) was refluxed under a nitrogen atmosphere for 11 h. Upon cooling to ambient temperature, the reaction mixture was shaken with diethyl ether (200 ml) and water (200 ml). The organic layer was dried with anhydrous $MgSO_4$ before evaporation to dryness. The crude product was purified by recrystallization from acetone to yield 2-(3-hydroxypropyl)-6-(4-cyanophenyl)naphthalene (2·10 g, 52 per cent). Proton NMR spectral data (in $CDCl_3$): δ 8·08–7·20 (m, 10 H, aromatic **H**), 4·51 (t, 2 H, CH_2 CH_2O(naphthyl)), 3·98 (t, 2 H, $HOCH_2CH_2$), δ 2·19 (p, 2 H, $CH_2CH_2CH_2$), 1·76 (s, 1 H, $HOCH_2$).

Using 4-hydroxy-4′-bromobiphenyl instead of 6-bromo-2-naphthol in the first step of the above procedures, one obtained the precursor to (**IV**) and (**V**), 4-(3-hydroxypropyl)-4″-cyanoterphenyl. Proton NMR spectral data (in $CDCl_3$): δ 7·81–7·00 (m, 12 H, aromatic **H**), 4·23 (t, 2 H, CH_2CH_2O(phenyl)), 3·94 (t, 2 H, $HOCH_2CH_2$), 2·13 (p, 2 H, $CH_2CH_2CH_2$), 1·72 (s, 1 H, $HOCH_2$).

2.2.2. *2-[4-[(3β-5-Cholestenyloxy)carbonyl]phenoxy] ethanol*

Based on Scheme 2, 4-methoxycarbonyloxybenzoic acid (2·54 g, 12·93 mmol) was dissolved in 25 ml dry methylene chloride with 5 drops *N,N*-dimethylformamide. Oxalyl chloride (1·75 ml, 20 mmol) was added to this solution, and the reaction mixture was stirred for 1·5 h before evaporating off the solvent and residual oxalyl chloride *in vacuo*. The resultant acid chloride was then dissolved in 20 ml dry THF, to which a solution containing cholesterol (4·99 g, 12·91 mmol), 20 ml dry THF, and 3 ml dry pyridine was added. The reaction mixture was stirred overnight, and most of the THF was then evaporated *in vacuo*. The solid residue was shaken with 150 ml methylene chloride and 150 ml water. The organic layer was dried over anhydrous $MgSO_4$, and the crude product obtained upon removing the solvent *in vacuo* was recrystallized from ethanol/acetone to yield (**A**) (5·53 g, 76 per cent). A solution containing (**A**) (5·49 g, 9·72 mmol) in 75 ml THF and 25 ml ethanol was prepared, to which 10 ml 30 per cent NH_4OH was added while stirring. The reaction mixture was then neutralized with 10 per cent HCl, and the solids were filtered off. The filtrate was shaken with 150 ml methylene chloride and 200 ml water. The organic layer was evaporated *in vacuo* to dryness, and the resultant solids were combined with the filtered solids to yield (**B**) (4·9 g, 100 per cent).

A solution was prepared by dissolving (**B**) (4·67 g, 9·217 mmol), Cs_2CO_3 (3·13 g, 9·594 mmol), and tetrahydropyran-protected 2-iodoethanol (2·96 g, 11·6 mmol) in 95 ml *N,N*-dimethylformamide. Upon stirring overnight at 60°C, the reaction mixture was poured into 500 ml water and then shaken with diethyl ether (3 × 100 ml). After drying the organic layer over anhydrous $MgSO_4$, the solvent was evaporated off *in vacuo*, and the crude product was recrystallized from ethanol to yield (**C**) (3·58 g, 61 per cent). In 40 ml THF plus 40 ml ethanol were dissolved (**C**) (4·00 g, 6·31 mmol) and pyridinium *p*-toluenesulphonate (0·146 g, 0·58 mmol). One drop of concentrated HCl was added, and the solution was stirred for 2 h at 60°C. The volume of the reaction mixture was then reduced to about 10 ml, which was then shaken with 150 ml methylene chloride and 100 ml water. Upon removing the solvent from the organic layer by evaporation *in vacuo*, the solid residue was recrystallized from ethanol/tetrahydrofuran to yield

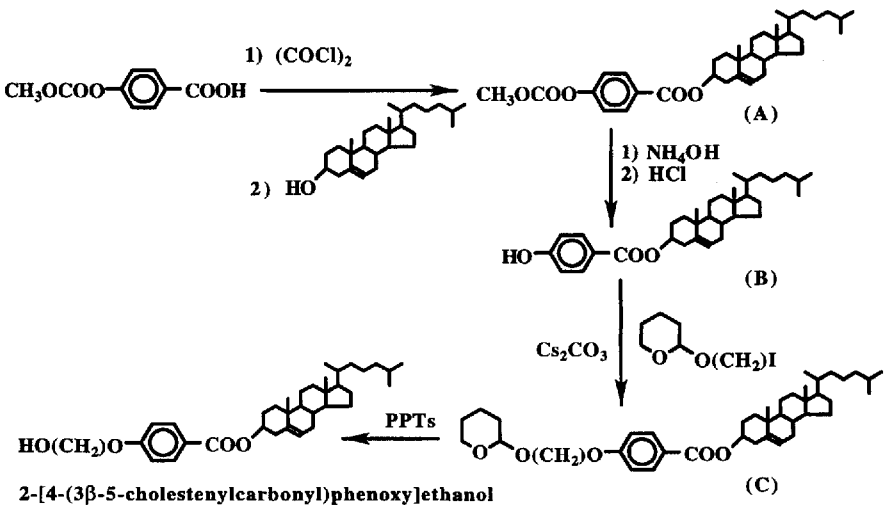

Scheme 2. Synthesis of 2-[4-(3β-5-cholestenylcarbonyl)phenoxy]ethanol.

2-[4-[(3β-5-cholestenyloxy)carbonyl]-phenoxy]ethanol (2·52 g, 72 per cent). Proton NMR spectral data (in $CDCl_3$): δ 8·04 (d, 2 H, aromatic **H**), 6·96 (d, 2 H, aromatic **H**), 5·25 (m, 1 H, C=C**H** in cholesterol), 4·87 (m, 1 H, COOC**H** in cholesterol), 4·17 (t, 2 H, CH_2CH_2O–(phenyl)), 4·10 (m, 2 H, $HOCH_2CH_2$), 2·48–0·66 (m, 53 H, cholesterol).

2.2.3. *Bicyclo[2.2.2]oct-7-ene-2,3,5,6-tetracarboxylic and trans-1,3,5-cyclohexanetricarboxylic acids*

Hydrolysis of bicyclo[2.2.2]oct-7-ene-2,3,5,6-tetracarboxylic dianhydride in boiling water followed by recrystallization from water yielded bicyclo[2.2.2]oct-7-ene-2,3,5,6-tetracarboxylic acid. Proton NMR (in DMSO-d_6), δ 11·92 (s, 4 H, carboxylic acid), 6·06 (d, 2 H, alkene), 2·99 (s, 6 H, overlap of bridgehead (2 H) and methine (4 H) signals]. Steiz's [24] procedure was followed to convert commercially available *cis*-1,3,5-cyclohexanetricarboxylic acid into a *trans* isomer with a 1-axial-2-equatorial configuration.

2.2.4. *1,3,5,7-Tetrakis(chlorocarbonyl)cubane*

Following the procedures reported by Eaton *et al.* [25], partial saponification of 1,4-bis(methoxycarbonyl) cubane and the subsequent Barton decarboxylation were accomplished to yield cubanecarboxylic acid, which was then converted to 1,3,5,7-tetrakis(chlorocarbonyl) cubane via photochemical chlorocarbonylation [26]. The overall yield was 34 per cent.

2.2.5. *Synthesis of compounds (**I**)–(**IV**), (**VI**), (**VIII**) and (**IX**) with procedures illustrated for (**III**)*

A solution containing 2-(3-hydroxypropyl)-6-(4-cyanophenyl)naphthalene (0·250 g, 0·825 mmol), *cis*-1,3,5-cyclohexanetricarboxylic acid (0·060 g, 0·278 mmol), and triphenylphosphine (0·255 g, 0·972 mmol) in 10 ml dry THF was prepared under a dry nitrogen atmosphere. Diethyl azodicarboxylate, DEAD, (0·175 g, 1·11 mmol) was then added dropwise, and the reaction mixture was stirred overnight at room temperature before evaporation *in vacuo* to dryness. The crude product was purified by flash column chromatography using methylene chloride/acetone (10:1) as the eluent. Further purification was accomplished by dissolving the solid residue in methylene chloride for precipitation into ethanol to yield (**III**) (0·249 g, 85 per cent).

2.2.6. *Synthesis of compound (**VII**)*

In 10 ml THF were dissolved 4-(3-hydroxypropyl)-4′-cyanobiphenyl (0·503 g, 1·986 mmol) and 1,3,5,7-tetrakis(chlorocarbonyl)cubane (0·175 g, 0·494 mmol). Dry pyridine (0·5 ml, 6·2 mmol) was added to the solution, and the reaction mixture was stirred at room temperature for 15 h. Then 10 ml THF was added, and the residual solids were filtered off. The volume of the filtrate was reduced to 8 ml via evaporation, and the crude product was collected by precipitation into 100 ml methanol. Purification was accomplished via flash column chromatography on silica gel using methylene chloride/acetone (20:1) as the eluent. Flash column chromatography was repeated to further purify the product using gradient elution from methylene chloride to methylene chloride/acetone (30:1) to yield (**VII**) (0·168 g, 28 per cent).

2.3. *Characterization techniques*

A Hitachi high performance liquid chromatography, HPLC, system comprising an L-2000 metering pump and an L-4200 UV-Vis absorbance detector equipped with an LiChrosorb® column (RP-18, 10 μm) was employed to determine the number of components and purity of the intermediates and products. The purity levels of all final products were found to be better than 99 per cent based on HPLC analysis. Chemical structures were elucidated with elemental analysis (performed by Oneida Research Services, Inc. in Whitesboro, New York), the FTIR (Nicolet 20 SXC) and proton NMR (QE-300, GE) spectroscopic techniques.

Thermal transition temperatures were determined by DSC (Perkin–Elmer DSC-7) with a continuous nitrogen purge at 20 ml min^{-1}. A heating rate of 20°C min^{-1} was normally employed to gather a thermogram with DSC unless noted otherwise. In the isothermal recrystallization experiment, the prior thermal history was eliminated by heating the sample to 20°C above its clearing point followed by quenching to −30°C at −200°C min^{-1}. The temperature for an isothermal experiment was then reached by heating at 20°C min^{-1}, and the sample was held there for a period of time for recrystallization to proceed to completion. A DuPont 951 thermogravimetric analyser interfaced with a DuPont Thermal Analyst 2100 System was used to perform TGA experiments at a nitrogen purge of 50 ml min^{-1} and a scan rate of 20°C min^{-1}. Morphology and liquid crystallinity were identified with a polarized optical microscope (Leitz Orthoplan-Pol), equipped with a hot stage (FP82, Mettler) plus a central processor (FP80, Mettler).

The X-ray diffraction data were collected in reflection mode geometry using a Siemens θ/θ Bragg–Brentano diffractometer utilizing nickel filtered Cu radiation and a Braun position sensitive detector set to measure CuKα radiation. This diffractometer was equipped with an Anton–Paar HTK temperature stage allowing for non-ambient data collection. Samples as fine powders were placed on a sample holder comprised of a platinum ribbon. This holder was heated using resistive heating. The temperature was monitored using a thermocouple positioned beneath the sample. Samples were heated in

a nitrogen atmosphere at 10°C min^{-1} before collecting diffraction data at the specified temperatures, each taking 5 min to complete.

3. Results and discussion

The nine model compounds synthesized for the present study are depicted in figure 1 with their chemical structures validated by elemental analysis and proton NMR spectral data compiled in tables 1 and 2, respectively. The stereochemical features, i.e. those of *cis*- and *trans*-1,3,5-cyclohexanetricarboxylate and *all-exo*-bicyclo[2.2.2]oct-7-ene tetracarboxylate, were identified with proton NMR spectroscopy as reported previously [21, 27]. Since thermal transition temperatures as determined by DSC are normally functions of prior thermal treatment and scanning rate as well, a consistent procedure was followed in which a sample was heated to beyond the clearing point, T_c, followed by quenching at -200°C min^{-1} to -30°C before running a heating scan at 20°C min^{-1}. Based on our prior experience with related liquid crystal compounds [17–20], thermal decomposition of the presently investigated compounds is not expected to occur at temperatures up to 250°C. The clearing temperatures of (**IV**) and (**V**) were observed at 307 and 277°C, respectively. However, from TGA heating scans a weight loss of 0·5 per cent at 350 and 330°C for (**IV**) and (**V**), respectively, indicated a thermal stability up to the reported T_cs. With hot-stage POM, nematic threaded textures were observed for all compounds upon heating through their respective transition temperatures except compound (**V**), for which the oily streaks characteristic of a cholesteric mesophase were observed. The so-obtained DSC thermograms of all compounds are presented in figure 2 which, combined with mesophase identification by hot-stage POM, yields thermotropic properties as indicated for all compounds. In what follows, the DSC and XRD data will be employed to assess the morphological stability of the quenched, mesomorphic glasses against thermally activated phase transformation.

Table 1. Elemental analysis of compounds (**I**) to (**IX**).

Compound		C/per cent	H/per cent	N/per cent
I	calcd.	74·25	5·58	4·56
	obsd.	74·12	5·65	4·50
II	calcd.	74·25	5·58	4·56
	obsd.	73·84	5·64	4·43
III	calcd.	77·29	5·36	3·92
	obsd.	76·90	5·42	3·81
IV	calcd.	78·31	5·52	3·65
	obsd.	77·78	5·64	3·56
V	calcd.	77·93	7·20	2·04
	obsd.	77·58	7·24	1·98
VI	calcd.	74·74	4·95	4·59
	obsd.	74·56	5·05	4·45
VII	calcd.	74·74	4·95	4·59
	obsd.	74·20	4·97	4·38
VIII	calcd.	74·50	5·26	4·57
	obsd.	74·28	5·33	4·57
IX	calcd.	78·68	4·40	3·82
	obsd.	78·59	4·58	3·82

As evidenced by glass transition upon heating the quenched glass, all compounds are capable of vitrification except (**IV**), which contains three linear cyanoterphenyl groups. An observation with hot-stage POM suggested that the isotropic melt of (**IV**) is quenched into a crystal, which is consistent with the isotropic→nematic→crystalline transition at 302 and 109°C as identified by the DSC cooling scan at -20°C min^{-1}. Based on XRD patterns presented in figure 3 together with the DSC heating scan shown in figure 2, it is clear that in the process of heating this crystal undergoes a crystalline modification at 132°C followed by a transition at 139°C into a nematic mesophase that turns into an isotropic melt at 307°C. It is remarked that the XRD patterns (see figure 3) are indicative of poorly ordered crystallites. In contrast, with two cyanoterphenyl and one cholesteryl groups, compound (**V**) turned out to be a glass-former with a cholesteric mesophase temperature range of more than 200°C. As evidence against morphological stability, the DSC heating scan of a mesomorphic glass would be expected to reveal a recrystallization exotherm followed by a crystalline melting endotherm. In a less obvious case, recrystallization upon heating may occur over such a wide temperature range that no exotherm appears in the heating scan. Even so, the accumulated crystals would result in a sharp crystalline melting point, T_m. These two cases are illustrated by the DSC thermograms of (**VI**) and (**IX**), respectively.

First of all, the DSC cooling scans of (**VI**) and (**IX**) at -20°C min^{-1} from 225 to 0°C showed no crystallization exotherms. A hot-stage POM observation of (**VI**) revealed that the two endotherms above the T_c of 150°C correspond to the melting of two crystalline forms. Specifically, heating the sample beginning at 110°C at a rate of 5°C min^{-1} resulted in a complete transformation (at 145°C) of the nematic melt into two distinct crystalline regions, which upon further heating at 1°C min^{-1} were found to undergo independent transitions into isotropic melts at 157 and 164°C, respectively. Further insight into the thermal transitions of (**VI**) was gained by gathering DSC heating scans at 10 and 40°C min^{-1} in addition to 20°C min^{-1} as compiled in figure 4. Three observations emerge from the 10°C min^{-1} scan shown as part of figure 4: (1) thermally activated recrystallization is represented by a broad exotherm at 143°C; (2) recrystallization has occurred literally to completion in view of a hardly visible nematic transition at 149°C;

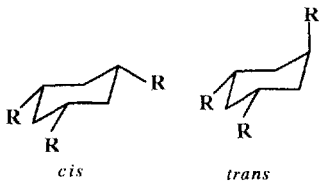

(I): *cis* with R = COO (C H_2)$_3$ O— —CN

(II): *trans* with R = COO (C H_2)$_3$ O— —CN

(III): *cis* with R = COO (C H_2)$_3$ O— —CN

(IV): *trans* with R = COO (C H_2)$_3$ O— —CN

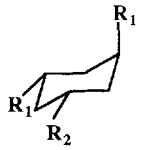

(V): *trans* with R_1 = COO (C H_2)$_3$ O— —CN

and R_2 = COO (C H_2)$_2$ O— —COO

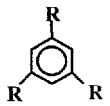

(VI): with R = COO (C H_2)$_3$ O— —CN

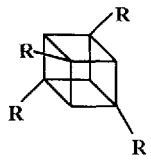

(VII): with R = COO (C H_2)$_3$ O— —CN

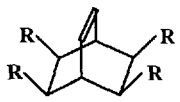

(VIII):*all-exo* with R = COO (C H_2)$_3$ O— —CN

(IX): *all-exo* with R = COO (C H_2)$_2$ O— —C≡C— —CN

Figure 1. Chemical structures of compounds (I) to (IX).

Table 2. Proton NMR spectral data in $CDCl_3$.

Compound	δ/ppm	Analysis
I	7·76–6·94	[m, 24 H, biphenyl aromatic]
	4·33	[t, 6 H, $COOCH_2CH_2$]
	4·10	[t, 6 H, CH_2CH_2O]
	2·52–2·25	[m, 6 H, *cis*-cyclohexane ring]
	2·16	[m, 6 H, $CH_2CH_2CH_2$]
	1·68–1·50	[m, 3 H, *cis*-cyclohexane ring]
II	7·78–6·94	[m, 24 H,biphenyl aromatic]
	4·36	[t, 2 H, $COOCH_2CH_2$ axial]
	4·30	[t, 4 H, $COOCH_2CH_2$ equatorial]
	4·10	[t, 6 H, CH_2CH_2O]
	3·01–1·48	[m, 15 H, $CH_2CH_2CH_2$ and *trans*-cyclohexane ring]
III	8·02–7·11	[m, 30 H, aromatic]
	4·35	[t, 6 H,$COOCH_2CH_2$ all equatorial]
	4·16	[t, 6 H, CH_2CH_2O]
	2·67–2·23	[m, 6 H, *cis*-cyclohexane ring]
	2·19	[m, 6 H, $CH_2CH_2CH_2$]
	1·70–1·50	[m, 3 H, *cis*-cyclohexane ring]
IV	7·85–6·92	[m, 36 H, terphenyl aromatic]
	4·38	[t, 2 H, $COOCH_2CH_2$ axial]
	4·32	[t, 4 H, $COOCH_2CH_2$ equatorial]
	4·10	[m, 6 H, CH_2CH_2O]
	3·05–1·52	[m, 15 H, $CH_2CH_2CH_2$ and *trans*-cyclohexane ring]
V	8·06–6·88	[m, 28 H, phenyl and terphenyl aromatics]
	5·41	[d, 1 H, alkene on cholesteryl group]
	4·83	[br, 1 H, CH(OOC) on cholesteryl group]
	4·50–4·00	[m, 12 H, $COOCH_2CH_2CH_2O$ on terphenyl groups and $COOCH_2CH_2O$ on cholesteryl group]
	3·00–0·60	[m, 66 H, 53 H on cholesteryl group, $CH_2CH_2CH_2$ on terphenyl groups and *trans*-cyclohexane ring]
VI	8·90	[s, 3 H, 1,3,5-benzene aromatic]
	7·75–6·94	[m, 24 H, biphenyl aromatic]
	4·64	[t, 6 H, $COOCH_2CH_2$]
	4·21	[t, 6 H, CH_2CH_2O]
	2·34	[p, 6 H, $CH_2CH_2CH_2$]
VII	7·84–6·94	[m, 32 H, biphenyl aromatic]
	4·66	[s, 4 H, 1,3,5,7-cubane group]
	4·39	[t, 8 H, $COOCH_2CH_2$]
	4·08	[t, 8 H, CH_2CH_2O]
	2·18	[p, 8 H, $CH_2CH_2CH_2$]
VIII	7·80–6·93	[m, 32 H, biphenyl aromatic]
	6·39	[m, 2 H,CH=CH]
	4·22	[m, 8 H, $COOCH_2CH_2$]
	4·08	[t, 8 H, CH_2CH_2O]
	3·39	[br, 2 H, CH, bridgehead]
	3·11	[s, 4 H, CH(COO), methine]
	2·09	[p, 8 H, $CH_2CH_2CH_2$]
IX	8·05–6·85	[m, 40 H, aromatic]
	6·43	[m, 2 H, CH=CH]
	4·39	[m, 8 H, $COOCH_2CH_2$]
	4·14	[t, 8 H, CH_2CH_2O]
	3·46	[br, 2 H, CH, bridgehead]
	3·19	[s, 4 H, CH(COO), methine]

and (3) the two endotherms at 157 and 163°C can be attributed to melting of the resultant crystals as observed under hot-stage POM. Furthermore, the XRD patterns at the same heating rate of 10°C min^{-1} between the selected temperatures, as shown in figure 5, are consistent with the above interpretation. Specifically, the crystals that melt at 157 and 163°C exhibit distinct diffraction patterns, as demonstrated by the XRD patterns at 150 and 160°C. In contrast, at a heating rate of 40°C min^{-1}, the DSC scan in figure 4 reveals neither a

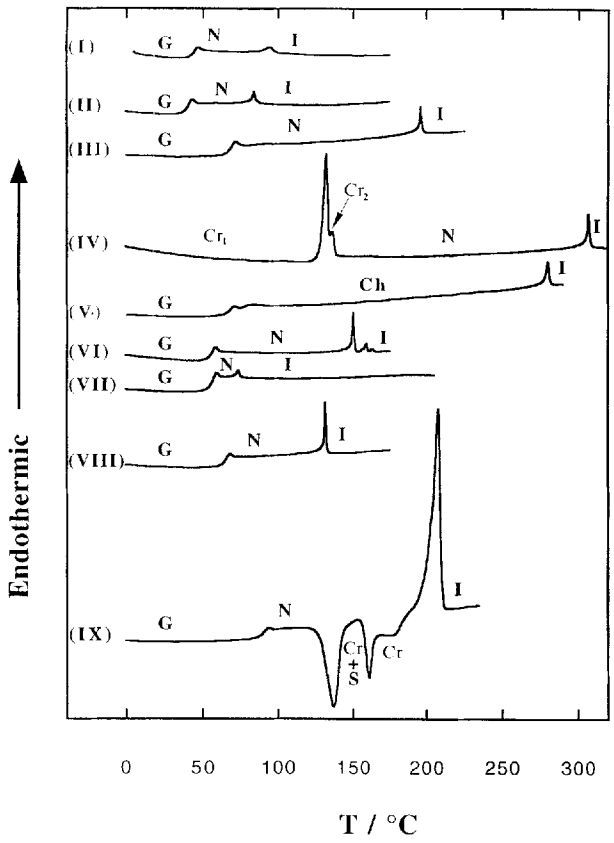

Figure 2. DSC thermograms of compounds (**I**) to (**IX**) at a standard heating rate of 20°C min^{-1}; samples preheated to beyond T_cs followed by quenching at −200°C min^{-1} to −30°C. Symbols: Cr, crystalline; Ch, cholesteric; S, smectic; N, nematic; and I, isotropic. The two endotherms above the clearing point of 150°C observed in compound (**VI**) are as interpreted in the text.

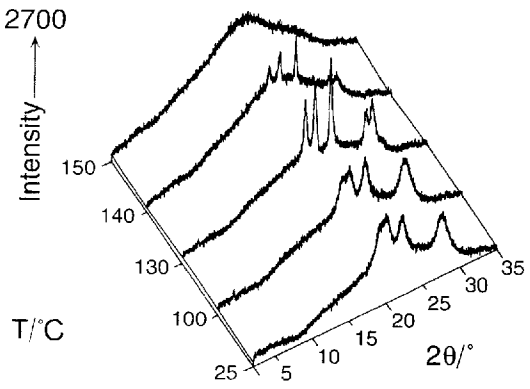

Figure 3. XRD patterns of the quenched glass of compound (**IV**) at selected temperatures; sample preheated to 320°C followed by quenching at −200°C min^{-1} to 25°C, and a heating scan of 10°C min^{-1} was adopted between the temperatures at which diffraction patterns were collected.

recrystallization exotherm nor a crystalline melting endotherm, implying a shortage of time at a faster scan rate for recrystallization to occur to an appreciable extent.

To better simulate the experimental condition of XRD, the DSC heating scan of (**IX**) at a heating rate of 10°C min^{-1} was obtained to locate the two exotherms at 118 and 143°C together with a T_g at 86°C, and a T_m at 206°C. It is noted that these transition temperatures differ from those observed at a standard DSC heating rate of 20°C min^{-1}, namely, 131 and 161°C with a T_g of 89°C and a T_m of 208°C as represented by the thermogram shown in figure 2. To elucidate the nature of the observed thermal transitions, XRD patterns across a temperature range from 115 to 175°C were collected in figure 6. In this temperature range, glass does not exist, and the broad diffraction peak centered at $2\theta = 20°$ is attributable to the nematic mesophase based primarily on the Schlieren texture observed with hot-stage POM. Note the minor crystalline diffraction pattern on top of the broad, nematic diffraction pattern at 115°C, indicating the onset of recrystallization from the nematic melt. The diffraction pattern at 125°C suggests the coexistence of smectic, crystalline, and residual nematic mesophase. Although the smectic texture was not readily identifiable in the presence of crystals, it was characterized by a series of three peaks at $2\theta < 7°$ corresponding to three orders of reflection with a periodicity of 5·6 nm. At 145°C the diffraction pattern shows the absence of a smectic mesophase with a much diminished residual nematic mesophase. Thus, the exotherm at 118°C can be attributed to nematic to smectic and crystalline transitions, and the one at 143°C smectic to crystalline transition. The fact that the crystalline patterns remain essentially identical at temperatures from 125 to 175°C suggests the presence of a single crystalline phase.

The applicability of DSC to qualitatively assessing the morphological stability of a quenched glass is further illustrated with the thermograms for (**I**) as presented in figure 7 showing an evidence of recrystallization not by the presence of an exotherm but of a crystalline melting endotherm at 153°C as a result of recrystallization at a heating rate of 2 and 0·5°C min^{-1}. A quenched glass with a better morphological stability is expected to undergo recrystallization at a slower heating rate. It was found that (**VII**) and (**VIII**) exhibit crystalline melting as a result of recrystallization at a heating rate of 1 and 0·2°C min^{-1}, respectively, whereas (**II**), (**III**) and (**V**) all show no evidence of recrystallization at a heating rate ranging from 0·2 to 40°C min^{-1}. Therefore, in terms of morphological stability, the following order is established for the nine model compounds: (**II**), (**III**), (**V**) > (**VIII**) > (**VII**) > (**I**) > (**VI**) > (**IX**) > (**IV**). It is evident that for a given pendant group the stereochem-

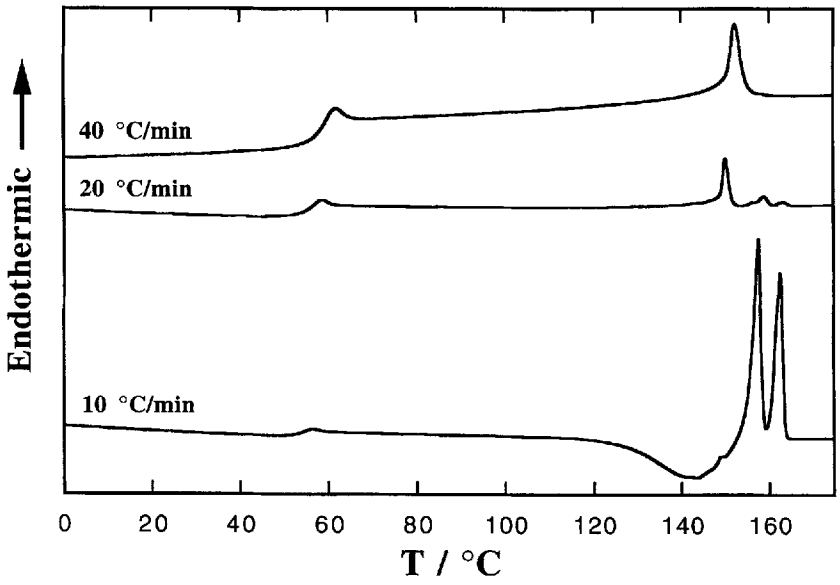

Figure 4. DSC thermograms of compound (**VI**) at a heating rate ranging from 10, 20 and 40°C min^{-1}; sample preheated to 200°C followed by quenching at −200°C min^{-1} to −30°C.

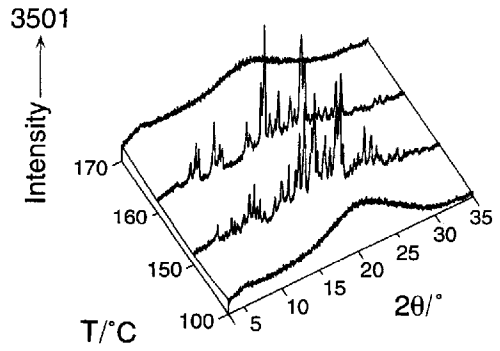

Figure 5. XRD patterns of the quenched glass of compound (**VI**) at selected temperatures; sample preheated to 200°C followed by quenching at −200°C min^{-1} to 25°C, and a heating scan of 10°C min^{-1} was adopted between the temperatures at which diffraction patterns were collected.

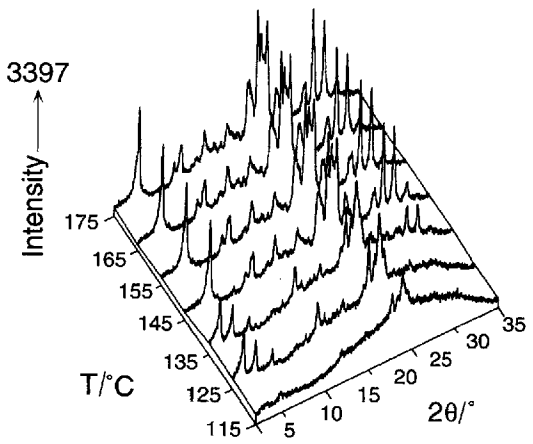

Figure 6. XRD patterns of the quenched glass of compound (**IX**) at selected temperatures; sample preheated to 240°C followed by quenching at −200°C min^{-1} to 25°C, and a heating scan of 10°C min^{-1} was adopted between the temperatures at which diffraction patterns were collected.

istry of the hybrid system plays an important role. Note that with *all-exo*-bicyclo[2.2.2]oct-7-ene as the central core, 1-phenyl-2-(6-cyanonaphth-2-yl)ethyne, a stronger nematogen [23, 28], i.e. with a higher T_c and a wider mesophase temperature range is inferior to the cyanobiphenyl group in terms of morphological stability. This is consistent with our previous observation [21] that a stronger nematogen is detrimental to morphological stability of the hybrid system. On the other hand, with *cis*-cyclohexane as the central core, the angular 6-(4-cyanophenyl)naphthyl group, also a stronger nematogen [23, 28], showed a comparable glass-forming ability to the cyanobiphenyl group, but the quenched glass of the former showed a morphological stability superior to that of latter. Thus, the glass-forming ability and morphological stability of the hybrid system seem to be determined by the nature of both the central core and the pendant nematogen and likely to be a consequence of a delicate structural balance between the two constituents.

An attempt was made to quantitatively evaluate morphological stability by performing an isothermal DSC experiment in which the enthalpy of recrystallization was monitored as a function of time. The half-time to complete recrystallization ($t_{1/2}$) was then determined via integration, a methodology frequently employed for the study of crystallization kinetics of polymeric materials [29, 30]. This technique was applied to compounds (**I**) and (**VI**), and the results are presented in figure 8 in

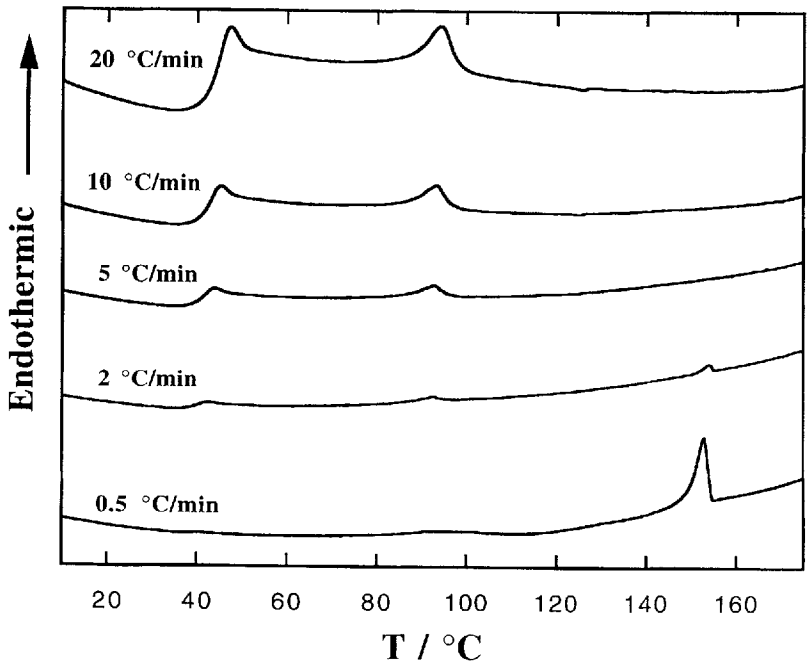

Figure 7. DSC thermograms of compound (**I**) at a heating rate ranging from 0·5 to 20°C min^{-1}; sample preheated to 200°C followed by quenching at −200°C min^{-1} to −30°C.

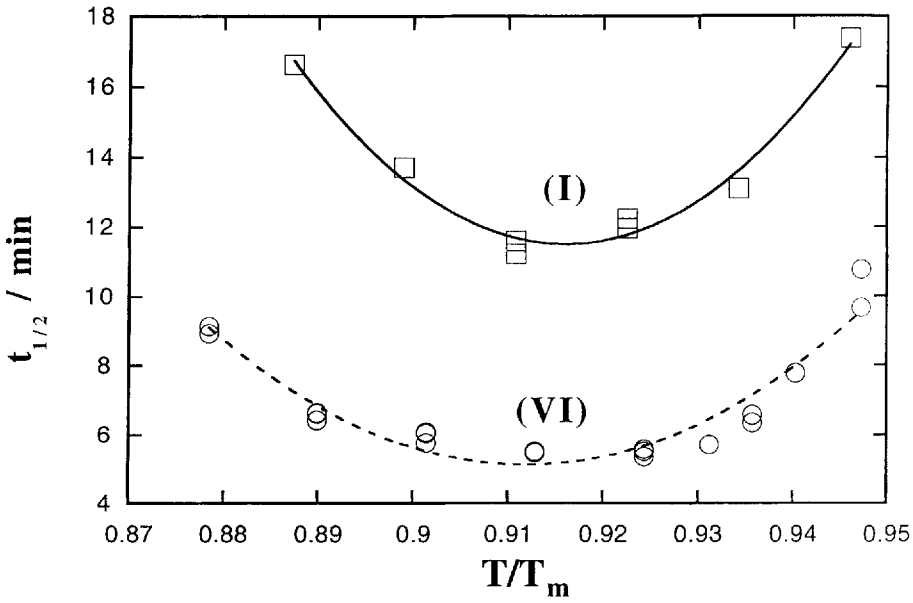

Figure 8. Half-time to complete recrystallization, $t_{1/2}$, as a function of T/T_m for compounds (**I**) and (**VI**) as determined by isothermal recrystallization using the DSC technique.

terms of $t_{1/2}$ as a function of reduced temperature, T/T_m (both in degrees Kelvin). Because of the disparity in thermal transition temperatures between different materials, it seems reasonable to compare the minimum $t_{1/2}$ and the temperature at which it occurs, $T(\text{min}.t_{1/2})$ relative to T_m of a given material, as a way to assess morphological stability. It was found that $\text{min}.t_{1/2}$ and $T(\text{min}.t_{1/2})$ are 11·5 min and 118°C for (**I**) and 5·1 min and 126°C for (**VI**). The ratios of $T(\text{min}.t_{1/2})$ to T_m turned out to be 0·918 and 0·915 for (**I**) and (**VI**) with a T_m of 153 and 163°C, respectively, which are identical within experimental error. In view of the temperature dependence of crystal growth rate, the observed equality of the reduced temperatures at minimum $t_{1/2}$s is significant in that it permits a sensible evaluation of morphological stability in terms of $\text{min}.t_{1/2}$. It is thus concluded that quenched glass (**I**) is more stable morphologically than quenched glass (**VI**), as also found from a qualitative assessment. Nonetheless, it should be pointed out that this quantitative approach is limited by the experi-

mentally accessible time-scale; compounds (**I**) and (**VI**) offered an optimum time scale for the reported isothermal recrystallization experiment using the DSC technique.

4. Conclusions

In summary, the present study has led to the following observations regarding the relationship between chemical structure, glass-forming ability and morphological stability:

(1) With cyanobiphenyl as the pendant nematogenic group, the morphological stability imparted by the central core to the hybrid system was established as follows: *trans*-cyclohexane > *all-exo*-bicyclo[2.2.2]oct-7-ene > cubane > *cis*-cyclohexane > benzene.

(2) Cyclohexane containing three cyanoterphenyl groups showed a strong tendency to crystallize upon quenching from the isotropic melt (i.e. lacking the ability to vitrify), but with the substitution of one of the cyanoterphenyl groups by a cholesteryl group, the resultant chiral nematic system showed superior glass-forming ability and morphological stability.

(3) With *cis*-cyclohexane as the volume-excluding central core, the angular 6-(4-cyanophenyl)naphthyl group, a stronger nematogen, showed a comparable glass-forming ability to the cyanobiphenyl group, but the quenched glass of the former showed a morphological stability superior to that of latter.

(4) With *all-exo*-bicyclo[2.2.2]oct-7-ene as the volume-excluding core, 1-phenyl-2-(6-cyanonaphth-2-yl)ethyne, a stronger nematogen, turned out to be inferior to the cyanobiphenyl group in terms of morphological stability of the quenched glass.

(5) A quantitative evaluation of the morphological stability of compounds (**I**) and (**VI**) was conducted by an isothermal recrystallization experiment across a temperature range from T_g to T_m using the DSC technique, which allows $t_{1/2}$ as a function of temperature to be determined. That the value of minimum $t_{1/2}$ of (**I**) is more than twice that of (**VI**) at the same reduced temperature indicates a superior morphological stability of (**I**).

We thank Professor A. S. Kende of the Chemistry Department at the University of Rochester for assistance in organic synthesis, Dr A. Schmid and Dr S. D. Jacobs of the Laboratory for Laser Energetics for helpful discussions. We would like to express our gratitude for the financial support provided by the Ministry of International Trade and Industry of Japan, Kaiser Electronics in San Jose, California, and the National Science Foundation under Grant CTS-9500737 and an Equipment Grant CTS-9411604. In addition, our advanced organic materials research was supported in part by the US Department of Energy Office of Inertial Confinement Fusion under Cooperative Agreement No. DE-FC03-92SF19460, the University of Rochester, and the New York State Energy Research and Development Authority. Financial support provided by the Armament Research, Development and Engineering Center to GEO-CENTERS, INC. is also gratefully acknowledged.

References

[1] Schadt, M., 1993, *Ber. Bunsen. Phys. Chem.*, **97**, 1213.
[2] (*a*) Ortler, R., Bräuchle, C., Miller, A., and Riepl, G., 1989, *Makromol. Chem. rap. Commun.*, **10**, 189; (*b*) Natarajan, L. V., Tondiglia, V., Bunning, T. J., Crane, R. L., and Adams, W. W., 1992, *Adv. Mater. Opt. Electr.*, **1**, 293.
[3] Eichler, H. J., Heppke, G., MacDonald, R., and Schmid, H., 1992, *Mol. Cryst. liq. Cryst.*, **223**, 159.
[4] Hirabayashi, K., and Kurokawa, T., 1993, *Liq. Cryst.*, **14**, 307.
[5] Loddoch, M., Marowsky, G., Schmid, H., and Heppke, G., 1994, *Appl. Phys. B*, **59**, 591.
[6] Smith, D. A. McL., and Coles, H. J., 1993, *Liq. Cryst.*, **14**, 937.
[7] Li. L., Yuan, H. J., and Palffy-Muhoray, P., 1994, *Liq. Cryst.*, **16**, 703.
[8] (*a*) Attard, G. S., Douglass, A. G., Imrie, C. T., and Taylor, L., 1992, *Liq. Cryst.*, **11**, 779; (*b*) Attard, G. S., and Imrie, C. T., 1992, *Liq. Cryst.*, **11**, 785.
[9] Kreuzer, F.-H., Andrejewski, D., Haas, W., Häberle, N., Riepl, G., and Spes, P., 1991, *Mol. Cryst. liq. Cryst.*, **199**, 345.
[10] (*a*) Singler, R. E., Willingham, R. A., Lenz, R. W., Furukawa, A., and Finkelmann, H., 1987, *Macromolecules*, **20**, 1727; (*b*) Allcock, H. R., and Kim, C., 1989, *Macromolecules*, **22**, 2596.
[11] Freidzon, Ya. S., D'yachenko, M. V., Tur, D. R., and Shibaev, V. P., 1993, *Polymer Preprints*, **34**, 146.
[12] Percec, V., Kawasumi, M., Rinaldi, P. L., and Litman, V. E., 1992, *Macromolecules*, **25**, 3851.
[13] Dehne, H., Roger, A., Demus, D., Diele, S., Kresse, H., Pelzl, G., Wedler, W., and Weissflog, W., 1989, *Liq. Cryst.*, **6**, 47.
[14] Schäfer, W., Uhlig, G., Zaschke, H., Demus, D., Diele, S., Kresse, H., Ernst, S., and Wedler, W., 1990, *Mol. Cryst. liq. Cryst.*, **191**, 269.
[15] Wedler, W., Demus, D., Zaschke, H., Mohr, K., Schäfer, W., and Weissflog, W., 1991, *J. mater. Chem.*, **1**, 347.
[16] Gresham, K. D., McHugh, C. M., Bunning, T. J., Crane, R. L., Klei, H. E., and Samulski, E. T., 1994, *J. Polym. Sci., Part A: Polym. Chem.*, **32**, 2039.
[17] Shi, H., and Chen, S. H., 1994, *Liq. Cryst.*, **17**, 413.
[18] Shi, H., and Chen, S. H., 1995, *Liq. Cryst.*, **18**, 733.
[19] Shi, H., and Chen, S. H., 1995, *Liq. Cryst.*, **19**, 849.
[20] Chen, S. H., Mastrangelo, J. C., Shi, H., Bashir-Hashemi, A., Li, J., and Gelber, N., 1995, *Macromolecules*, **28**, 7775.
[21] Shi, H., and Chen, S. H., 1995, *Liq. Cryst.*, **19**, 785.
[22] Mastrangelo, J. C., and Chen, S. H., 1993, *Macromolecules*, **26**, 6132.
[23] Hird, M., Toyne, K. J., Gray, G. W., Day, S. E., and McDonnell, D. G., 1993, *Liq. Cryst.*, **15**, 123.

[24] STEIZ, A. JR., 1968, *J. org. Chem.*, **23,** 2978.
[25] EATON, P. E., NORDARI, N., TSANAKTSIDIS, J., and UPADHYAYA, S. P., 1995, *Synthesis*, 501.
[26] (*a*) BASHIR-HASHEMI, A., 1993, *Angew. Chem. Int. Ed. Engl.*, **32,** 612; (*b*) BASHIR-HASHEMI, A., LI, J., GELBER, N., and AMMON, H., 1995, *J. org. Chem.*, **60,** 698.
[27] MASTRANGELO, J. C., CHEN, S. H., and BLANTON, T. N., 1995, *Chem. Mater.*, **7,** 1904.
[28] WU, S-T., RAMOS, E., and FINKENZELLER, U., 1990, *J. appl. Phys.*, **68,** 78.
[29] CAMPOY, I., MARCO, C., GÓMEZ, M. A., and FATOU, J. G., 1992, *Macromolecules*, **25,** 4392.
[30] LIM, G. B. A., and LLOYD, D. R., 1993, *Polym. Eng. Sci.*, **33,** 513.